

Quantum state reconstruction using binary data from on/off photodetection

Giorgio Brida, Marco Genovese, Marco Gramegna, Alice Meda, Fabrizio Piacentini, Paolo Traina
I.N.R.I.M., Strada delle Cacce 91, Torino, Italia

Enrico Predazzi
INFN and Dipartimento di Fisica Teorica, Universit'a di Torino, I-10125 Torino, Italia

Stefano Olivares, Matteo G. A. Paris
*CNISM UdR Milano Universit'a, I-20133 Milano, Italia and
Dipartimento di Fisica dell'Universit'a degli Studi di Milano, I-20133 Milano, Italia*
(Dated: November 1, 2018)

The knowledge of the density matrix of a quantum state plays a fundamental role in several fields ranging from quantum information processing to experiments on foundations of quantum mechanics and quantum optics. Recently, a method has been suggested and implemented in order to obtain the reconstruction of the diagonal elements of the density matrix exploiting the information achievable with realistic on/off detectors, e.g. silicon avalanche photo-diodes, only able to discriminate the presence or the absence of light. The purpose of this paper is to provide an overview of the theoretical and experimental developments of the on/off method, including its extension to the reconstruction of the whole density matrix.

PACS numbers: 03.65.Wj, 42.50.Ar, 45.50.Dv, 42.62.Eh

I. INTRODUCTION

The knowledge of the density matrix of a quantum state is fundamental for several applications, ranging from quantum information [1] to the foundations of quantum mechanics [2] and quantum optics [3–10]. In turn, many efforts have been devoted to find reliable methods to fully or partially reconstruct the density matrix especially. This is especially true for the density matrix in the photon number basis, and in this case the reconstruction of the diagonal elements, i.e. the photon statistics, is of great relevance for the characterization and use of the state in quantum communication and information processing. In fact, the field of photodetection has received much attention in the last decades, however, the choice of a detector with internal gain suitable for the measurement is still a non trivial task when the flux of the photons to be counted is such that more than one photon is detected in the time-window of the measurement, which in turn is set by the detector pulse-response, or by an electronic gate on the detector output, or by the duration of the light pulse. In this case, we need a congruous linearity in the internal current amplification process: each of the single electrons produced by the different photons in the primary step of the detection process (either ionization or promotion to a conduction band) must experience the same average gain and this gain must have sufficiently low spread. The fulfillment of both requisites is necessary for the charge integral of the output current pulse be proportional to the number of detected photons. Photon detectors that can operate as photon counters are rather rare [11, 12]. Among these, Photo-Multiplier Tubes (PMT's) [13, 14] and hybrid photo-detectors [15, 16] have the drawback of a low quantum efficiency, since the detection starts with the

emission of an electron from the photo-cathode. Solid state detectors with internal gain, in which the nature of the primary detection process ensures higher efficiency, are still under development. Highly efficient thermal photon counters have also been used, though their operating conditions are still extreme (cryogenic conditions) to allow common use [17–19]. Better results can be in principle be obtained using photon chopping in conjunction with single-photon detectors, whereas the experimental implementation of loop-detectors has shown interesting performances. The advent of quantum tomography provided an alternative method to measure photon number distributions [20, 21]. However, the tomography of a state, which has been applied to several quantum states [9, 22–25], needs the implementation of homodyne detection, which in turn requires the appropriate mode matching of the signal with a suitable local oscillator at a beam splitter. Such mode matching is a particularly challenging task in the case of pulsed optical fields.

Photodetectors that are usually employed in quantum optics such as Avalanche Photo-Diodes (APD's) operating in the Geiger mode [18, 26–28] appears, at a first sight, to be definitely useless as photon counters. They are the solid state photo-detectors with the highest quantum efficiency and the greatest stability of the internal gain. However, they have the obvious drawback that the breakdown current is independent of the number of detected photons, which in turn cannot be determined. The outcome of these APD's is either "off" (no photons detected) or "on" *i.e.* a click indicating the detection of one or more photons. Actually, such an outcome can be provided by any photodetector (PMT, hybrid photodetector, cryogenic thermal detector) for which the charge contained in dark pulses is below that of the output current pulses corresponding to the detection of at least one

photon. Notice that for most high-gain PMT's the anodic pulses corresponding to no photons detected can be easily discriminated by a threshold from those corresponding to the detection of one or more photons. Despite the above considerations, a certain effort has been devoted to the reconstruction of the photon distribution from realistic detectors [33–37], and an effective method to reconstruct the photon distribution starting from on/off photodetection has been suggested [29–31], developed [32], and implemented in the last five years [38, 39, 41–44]. Convincing results have been obtained for the reconstruction of the photon distribution of both single- and bi-partite quantum optical states, thus showing that an appropriate data processing may turn APD into a powerful tool for quantum state reconstruction. The technique has been later extended to the reconstruction of the entire density matrix, including the off-diagonal elements [52].

The purpose of this paper is to review the theoretical basis of the on/off method, and of its experimental implementations, as well as its application to the reconstruction of the density matrix in different optical regimes. The paper is structured as follows. In Section II we give an overview on the method focusing on the reconstruction of the photon distribution for single-mode states. Section III describes the extension of the method to the bipartite case and report experimental implementation and results. In Section IV we describe how the method can be extended to achieve the reconstruction of the whole density matrix and report some recent experimental results about the reconstruction of the quantum state of light from coherent and pseudo-thermal sources. Finally, Section V closes the paper with some concluding remarks and summarizing future perspectives.

II. ON/OFF RECONSTRUCTION OF THE PHOTON DISTRIBUTION

Let us consider a single-mode quantum optical state. All the accessible information on the state can be obtained using the Born trace rule on its *density matrix* ρ , which, in the photon number basis reads as follows

$$\rho = \sum_{n,m=0}^{\infty} \rho_{nm} |n\rangle\langle m| \quad (1)$$

In particular, the information about the photon distribution of the state is given by the diagonal elements $\rho_n \equiv \rho_{nn}$ of the density matrix.

In this Section we are going to show how reconstruction of the ρ_n 's for a general quantum optical state is possible upon exploiting the set of binary data obtained by a two-level, on/off, detector. We assume that our state is revealed by a detector like silicon APDs (avalanche photo-diodes) or a photomultiplier operating in Geiger mode, i.e. a detector discriminating only between the absence of the presence of the light with a quantum efficiency $0 \leq \eta \leq 1$. If we label by 0 (off) and 1 (on) the

two possible outcomes, the overall measurement process for this kind of detector may be described by a two-value *positive operator-valued measure* (POVM) of the form

$$\Pi_0(\eta) = \sum_{n=0}^{\infty} (1-\eta)^n |n\rangle\langle n|, \quad \Pi_1(\eta) = \mathbf{I} - \Pi_0(\eta). \quad (2)$$

The off probability, $p_0 = \text{Tr}[\rho \Pi_0(\eta)]$, is thus given by:

$$p_0(\eta) = \sum_{n=0}^{\infty} (1-\eta)^n \rho_n = \sum_{n=0}^{\infty} A_n(\eta) \rho_n, \quad (3)$$

and the detection probability by $p_1(\eta) = 1 - p_0(\eta)$. We assume to have the possibility of varying the quantum efficiency η of our detector and to perform K on/off measurements, each one with a different η . The set of experimental data will thus a sample from the overall distribution

$$\mathbf{P}_0 \equiv \left\{ p_\mu : p_\mu = \sum_{n=0}^{\infty} A_{\mu n} \rho_n \quad \mu = 1, \dots, K \right\} \quad (4)$$

where we have defined $A_{\mu n} \equiv A_n(\eta_\mu)$. According to the normalization condition of quantum states we may always assume $\rho_n \simeq 0, \forall n > N$ for some N . Eq. (4) may be thus rewritten as a linear system:

$$\mathbf{P}_0 = \mathbb{A} \cdot \boldsymbol{\rho} \quad \boldsymbol{\rho} \equiv \{\rho_1, \dots, \rho_N\} \quad (5)$$

where the matrix of coefficients \mathbb{A} is a nonsingular Vandermonde matrix of order $N + 1$, whose coefficients are the geometric progression $(1 - \eta_\mu)^n$.

The simplest way to extract the photon distribution from the above relation is of course via matrix inversion. On the other hand, the form of the matrix \mathbb{A} is such that numerical inversion with \mathbf{P}_0 substituted by the experimental frequencies \mathbf{F}_0 is highly inefficient, i.e it would require a huge number of experimental runs to avoid large numerical fluctuations. The need of a faster and statistically more reliable solution thus arises. A closer look to Eq. (5) reveals that it represents as a linear positive (LINPOS) statistical model for the unknowns ρ_n coefficients, which may be effectively solved by means of a maximum likelihood (ML) approach, i.e. upon finding the ρ_n 's there are most likely to produce the observed data. If n_μ is the total number of experimental runs performed with quantum efficiency η_μ and $n_{0\mu}$ the registered number of off events, then the overall probability, i.e. the likelihood, of the observed sample is given by $\mathcal{L} = p_0(\eta_\mu)^{n_{0\mu}} (1 - p_0(\eta_\mu))^{n_\mu - n_{0\mu}}$. Upon, using the expectation maximization (EM) algorithm [45] to maximize the likelihood functional (actually the log-likelihood $L = \log \mathcal{L}$), and imposing the normalization constraint $\sum_n \rho_n = 1$, we arrive at the iterative formula

$$\rho_n^{(i+1)} = \rho_n^{(i)} \sum_{\mu=1}^K \left[\frac{A_{\mu n}}{\sum_{\lambda=1}^K A_{\lambda n}} \frac{f_\mu}{p_\mu \left[\left\{ \rho_n^{(i)} \right\} \right]} \right] \quad (6)$$

where $\{\rho_n^{(i)}\}$ is the distribution as reconstructed at the i -th step of the iterative algorithm, $f_\mu = n_{0\mu}/n_\mu$ is the experimental frequency of the off event with quantum efficiency η_μ , and $p_\mu \left[\left\{ \rho_n^{(i)} \right\} \right]$ is the probability of the off event with quantum efficiency η_μ , as evaluated using the distribution $\{\rho_n^{(i)}\}$ at the i -th step [31].

The formula in Eq. (6) allows one to reconstruct the photon distribution in terms of experimental off frequencies f_μ and, of course, of the values of the quantum efficiencies η_μ themselves. Being an iterative algorithm, the need of a measure of convergence arises. This may be obtained either checking whether it effectively leads to a maximum for the likelihood functional or, alternatively, upon introducing an error parameter $\epsilon^{(i)}$, defined as the distance between the experimental off frequencies and the corresponding probability reconstructed at the i -th step,

$$\epsilon^{(i)} = K^{-1} \sum_{\mu=1}^K \left| f_\mu - p_\mu \left(\left\{ \rho_n^{(i)} \right\} \right) \right|. \quad (7)$$

In fact, the error $\epsilon^{(i)}$ effectively measures how well the reconstructed distribution reproduces the observed data. In turn, we found excellent results upon stopping the iteration number when the value of $\epsilon^{(i)}$ goes below a certain threshold quantifying the overall precision of the reconstruction.

In order to assess the accuracy of the method, we consider a measure of fidelity for the reconstructed photon distribution in comparison to the theoretical one or expected one $\rho_n^{(th)}$, as follows

$$G^{(i)} = \sum_{n=0}^N \sqrt{\rho_n^{(th)} \rho_n^{(i)}}. \quad (8)$$

Several simulated experiments have shown the reliability of the method, which is also robust against fluctuations in the values of the quantum efficiencies η_μ . This is a crucial feature for the experimental implementation of the method, where the values η_μ are unavoidably determined within some confidence interval, and may fluctuate during the experimental runs.

Since the maximum likelihood method provides an asymptotically unbiased estimator, the confidence interval on the determination of the element $\rho_n^{(i)}$ can be estimated, for large number of measurements, in terms of the variance:

$$\sigma_n^2 = (K F_n)^{-1} \quad (9)$$

being F_n the Fisher information:

$$F_n = \sum_{\mu=1}^K \frac{1}{l_\mu} \left(\left. \frac{\partial l_\mu}{\partial \rho_n} \right|_{\rho_n = \rho_n^{(i)}} \right)^2 \quad (10)$$

where

$$l_\mu = \frac{\sum_{n=0}^N A_{\mu n} \rho_n}{\sum_{\mu=1}^K \sum_{n=0}^N A_{\mu n} \rho_n}.$$

As a first example of experimental reconstruction, we consider a weak coherent state generated by a cw He-Ne laser emission and detected by an APD. The maximum quantum efficiency is given by the nominal efficiency of the detector, i.e. $\eta = 0.66$, whereas the lower values of η needed by the algorithm are obtained by inserting neutral filters on the optical path of the signal beam. In the upper panel of Fig.1 we show the reconstructed photon number distribution, compared to a Poissonian distribution with the same mean value. In turn, a best fit procedure shows that the reconstructed photon number distribution is compatible with the one expected for a coherent state with a mean number of photons equal to $\langle n \rangle = 5.39$. We also show the convergence of the algorithm: the inset in the upper panel shows the log-likelihood L as a function of the number of steps of the iterative formula whereas in the lower panel we report the error parameter $\epsilon^{(i)}$ and the fidelity $G^{(i)}$ as a function of the number of steps. At convergence we have fidelity $G \gtrsim 0.995$ between the reconstructed distribution and the expected Poissonian.

As a second example, we consider an experiment where single-photon states are generated by means of a PDC heralding technique [38, 39]. In this scheme, a pair of correlated photons of different polarization are produced by pumping a type-II β -barium-borate (BBO) crystal with a CW argon ion laser beam (351 nm) in collinear geometry. After having split the photons of the pair by means of a polarizing beam splitter, the detection of one of the two by a silicon avalanche photodiode detector (SPCM-AQR-15, Perkin Elmer) is used to herald the presence of the second photon in the other channel, that is a window of 4.9 ns is opened for detection in the second arm, in correspondence to the detection of a photon in arm 1. This heralded photon is then measured by another APD (SPCM-AQR-15, Perkin Elmer) preceded by an iris and an interference filter (IF) centered at 702 nm (4 nm of FWHM) inserted with the purpose of reducing the noise due to the stray light. The overall quantum efficiency of the detection apparatus is $\eta = 20\%$ (estimated by Klyshko method [40?]), whereas lower quantum efficiencies are obtained by inserting calibrated neutral filters (NF) on the optical path of the heralded photon.

The reconstructed photon distribution is excellent agreement with the expected one: together with a dominant single photon component, a vacuum, $\rho_0 = 0.027 \pm 0.002$, and double pair $\rho_2 = 0.019 \pm 0.002$ components have been obtained. Those are quantitatively in agreement with the expectations, due to a small rate of dark counts in the heralding detector, which trigger the measurement in absence of the heralded photon, and to the presence of a small multiphoton component in the PDC output. Finally, we mention a recent experiments, where the method was applied to the reconstruction of the photon distribution of one arm of stimulated PDC, i.e. PDC with a coherent seed in the signal mode [46]. In this case, a generalized version of the reconstruction algorithm have been developed, which allows us to include constraints on

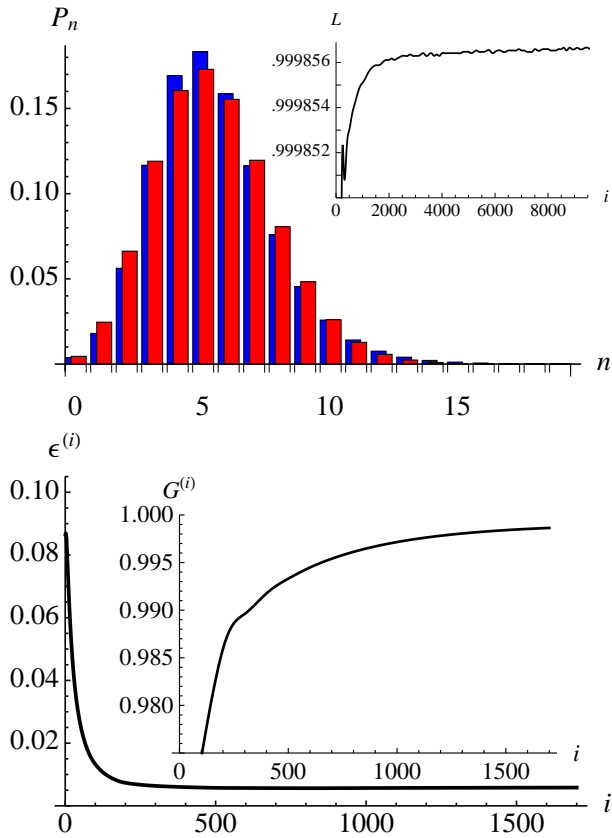


FIG. 1: On/off reconstruction of single-mode states. The upper panel shows the reconstruction of the photon distribution for a weak coherent state (blue) compared to a Poissonian distribution (red) with the same mean value. The data corresponds to a coherent state with a mean number of photons $\langle n \rangle = 5.39$. The inset shows the behaviour of the -log-likelihood L as a function of the number of steps of the iterative algorithm. In the lower panel we show the behaviour of the error parameter $\epsilon^{(i)}$ and of the fidelity $G^{(i)}$ as a function of the number of steps of the iterative algorithm.

specific moments, and it has been shown that it provides very good reconstruction in critical cases.

III. EXTENSION TO THE BIPARTITE CASE

Multimode states often occur in quantum optical implementations of quantum information processing, either because of the intrinsic properties of the involved interactions, or for the need of the specific application. In turn, in this Section, our aim is to present the extension of our method to the multimode case. In particular, we focus attention to the bipartite case and present the results of a set of experiments, performed to reconstruct the joint photon distribution of the two modes exiting a beam splitter [42]. In order to generalize the formulas of the previous Section we assume to deal with a pair of modes that are detected by two on/off detectors. There are four possible outcomes, which occur with the follow-

ing probabilities

$$\begin{cases} p_{00}(\eta) = \sum_{n,k} A_n(\eta)A_k(\eta)\varrho_{nk} \\ p_{01}(\eta) = \sum_{n,k} A_n(\eta)[1 - A_k(\eta)]\varrho_{nk} \\ p_{10}(\eta) = \sum_{n,k}[1 - A_n(\eta)]A_k(\eta)\varrho_{nk} \\ p_{11}(\eta) = 1 - p_{00}(\eta) - p_{10}(\eta) - p_{01}(\eta) \end{cases} \quad (11)$$

where:

$$\varrho_{nk} = \langle nk | \varrho | nk \rangle \quad |nk\rangle = |n\rangle \otimes |k\rangle \quad (12)$$

is the joint photon distribution of the bipartite state, i.e. the diagonal elements of the four-index two-mode density matrix, and η is the quantum efficiency of the photodetectors, which we assume to be identical. The above equations provide a relation between the statistics of the clicks of the two detectors and the actual statistics of photons. Upon assuming, because of the normalization, that the elements $\varrho_{nk} \simeq 0$ are negligible beyond some threshold $\forall n, k \geq N$, we may work in a (bipartite) truncated $(N+1) \times (N+1)$ Hilbert space. Again, if we can properly change the quantum efficiency of our system in such a way that K different measurements can be performed (with K different values η_μ , $\mu = 1, \dots, K$, ranging from $\eta_1 = \eta_{\min}$ to a maximum value $\eta_K = \eta_{\max}$), the whole amount of on/off detection statistics collected may give enough information to reconstruct the joint photon distribution of the bipartite state.

In more details, by re-ordering the diagonal matrix elements according to the rule

$$\varrho_{nk} \rightarrow q_p \quad p = 1 + k + n(1 + N)$$

we may define the vectors

$$\mathbf{g} = (p_{00}^{\eta_1}, \dots, p_{00}^{\eta_K}, p_{01}^{\eta_1}, \dots, p_{01}^{\eta_K}, p_{10}^{\eta_1}, \dots, p_{10}^{\eta_K}) \quad (13)$$

$$\mathbf{q} = (\varrho_{00}, \varrho_{01}, \varrho_{10}, \dots) \quad (14)$$

and thus summarize the on/off statistics with the compact formula:

$$g_\mu = \sum_{p=1}^{(N+1)^2} B_{\mu p} q_p \quad \mu = 0, \dots, 3K$$

that is

$$\mathbf{g} = \mathbb{B} \cdot \mathbf{q} \quad (15)$$

where we have introduced the matrix \mathbb{B} with entries:

$$[\mathbb{B}]_{\mu p} = \begin{cases} A_{\mu n} A_{\mu k} & \mu = 1, \dots, K \\ A_{\mu n} (1 - A_{\mu k}) & \mu = K + 1, \dots, 2K \\ (1 - A_{\mu n}) A_{\mu k} & \mu = 2K + 1, \dots, 3K \end{cases} \quad (16)$$

where, inverting the transformation rule introduced above, we have $k = (p - 1) \bmod (1 + N)$ and $n = (p - 1 - k) / (1 + N)$.

Eq. (15) represents a finite statistical linear model for the positive unknown q_p . As for the single-mode case we may solve the model using a ML approach and, in particular, we may use EM algorithm to obtain an iterative solution of the maximization problem

$$q_p^{(i+1)} = q_p^{(i)} \sum_{\mu=1}^{3K} \left[\frac{B_{\mu p}}{\sum_{\lambda} B_{\lambda p}} \frac{h_{\mu}}{g_{\mu}[\{q_p^{(i)}\}]} \right], \quad (17)$$

where $q_p^{(i)}$ denotes the p -th element of the reconstructed joint distribution, $g_{\mu}[\{q_p^{(i)}\}]$ are the detection probability reconstructed at the i -th step and h_{μ} are the experimental frequencies of the off events, i.e

$$h_{\mu} = \begin{cases} f_{00} = n_{00\mu} / n_{\mu} & \mu = 1, \dots, K \\ f_{01} = n_{01\mu} / n_{\mu} & \mu = K + 1, \dots, 2K \\ f_{10} = n_{10\mu} / n_{\mu} & \mu = 2K + 1, \dots, 3K \end{cases} \quad (18)$$

being $n_{01\mu}, n_{10\mu}, n_{00\mu}$ the number of single and double off events observed on the whole amount n_{μ} of experimental runs performed with $\eta = \eta_{\mu}$.

In order to evaluate the confidence interval on the determination of the element $q_p^{(i)}$ we still use eq. (9), but now the Fisher information F_p is rewritten as

$$F_p = \sum_{\mu=1}^{3K} \frac{1}{d_{\mu}} \left(\frac{\partial d_{\mu}}{\partial q_p} \Big|_{q_p=q_p^{(i)}} \right)^2 \quad (19)$$

with

$$d_{\mu} = \frac{\sum_{p=1}^{(N+1)^2} B_{\mu p} q_p}{\sum_{\mu=1}^{3K} \sum_{p=1}^{(N+1)^2} B_{\mu p} q_p}.$$

The analogous of the total error $\epsilon^{(i)}$ of Eq. (7) is given by $\epsilon^{(i)} = (3K)^{-1} \sum_{\mu=1}^{3K} \left| h_{\mu} - g_{\mu}[\{q_p^{(i)}\}] \right|$, which measures the distance of the reconstructed off probabilities from the measured frequencies. Also for the two-mode case, the algorithm may stopped when $\epsilon^{(i)}$ achieves a minimum or goes below a certain threshold value. Finally, the fidelity equation (8) for the reconstructed joint photon number distribution may be generalized $G^{(i)} = \sum_{p=1}^{(N+1)^2} \sqrt{q_p^{(th)} q_p^{(i)}}$ giving us the chance to compare the obtained $q_p^{(i)}$ with the expected ones ($q_p^{(th)}$).

Let us now report the experimental results obtained by applying the reconstruction method presented above to two different bipartite states. The first is the state obtained with a single photon state passing through a beam splitter (BS), whereas the second corresponds to the splitting of a PDC single branch. In both cases, which corresponds to very different optical regimes, the algorithm provides good reconstruction of the joint photon distribution [42, 43].

In our first experimental setup, see Fig. 2, [42], a 0.2 W, 398 nm pulsed (with 200 fs pulses and 70 MHz repetition rate) laser pump have been generated by second harmonic of a Ti:Sapphire laser at 796 nm and then injected into a $5 \times 5 \times 1$ mm type-II BBO crystal, this leading to the generation of entangled photon pairs by parametric downconversion. The detection of a photon on one of two correlated branches of degenerate PDC emission is used as trigger to herald the presence of the correlated photon in the other direction.

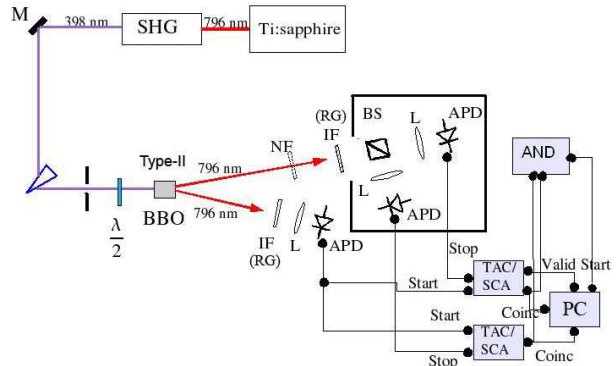


FIG. 2: On/off reconstruction of two-mode states. Schematic diagram of the experimental setup realizing the type-II PDC heralded photon source used to generate a two-mode superposition of a single-photon state with the vacuum. The idler photon is addressed to an IF (RG) filter, collected and sent to APD1, opening a coincidence window in the TAC modules; the signal goes through the NF and the IF (RG) filters, and then is split by the BS, whose outputs are collected and sent to APD2 and APD3 to close the coincidence windows. The output of the two TACs is also sent to an AND logical gate whose outputs gives the number of double coincidences.

The idler photon is addressed to an optical filter (a narrow band interference filter or a red glass, as will be specified later), collected by a lens and finally sent to a silicon APD (APD1). The corresponding signal is properly filtered (with the same filter as the idler photon) and then sent into a beam splitter (BS), separating in two the optical path of the photon and thus generating a bipartite state, that is the nonlocal superposition of a single photon state and the vacuum in the two arms

$$|\psi_{BS}\rangle = \sqrt{\tau}|0\rangle|1\rangle + \sqrt{1-\tau}|1\rangle|0\rangle \quad (20)$$

where τ is the BS transmittance. The BS is followed, on both output arms, by a collection/detection apparatus, denoted by APD2 and APD3, of the same type as APD1 (all the detectors were Perkin Elmer SPCM-AQR-15 silicon APDs). The proper set of quantum efficiencies are obtained by inserting, before the BS, several neutral filters (NF) of different transmittance, calibrated by measuring the ratio between the counting rates on D2 and D3 with the filter inserted and without it. In correspondence of the detection of a photon in arm 1, a coincidence window is opened on both detectors on arm 2: this may be obtained by sending the output of D1 as

Start to two Time-to-Amplitude Converters (TAC) that received the detector signal of D2 and D3 as stop. The 20 ns coincidence window has been set such to avoid spurious coincidences with PDC photons belonging to the following pulse (we remind that the repetition rate of the laser is 70 MHz). The TAC outputs are then addressed to the computer and to an AND logical gate in order to reveal coincidences between them; its output is also collected via computer, together with one TAC's valid start, giving us the total number of opened coincidence windows. These four data sets allow evaluating the frequencies f_{00} , f_{01} , f_{10} , f_{11} , needed for the reconstruction of the photon statistics. The background is estimated and subtracted by measuring the TACs and AND outputs out of the window triggered by APD1 detection. The maximum quantum efficiency is evaluated as the ratio between the sum of coincidences in APD2 and APD3 and the counting rate on APD1 without the insertion of any NF [48, 49]. In order to verify the method in different conditions we have also considered four alternatives given by the combination of a balanced (50% - 50%) or unbalanced (40% - 60%) BSs with two optical filters sets, either large band red glass filters (RG) with cut-off wavelength at 750 nm, or interference filters (IF) with peak wavelength at 796 nm and a 10 nm FWHM. The first test has been performed with the 50%-50% BS and the interference filters, for which we have collected data for $K = 33$ different quantum efficiencies. Elaborating these data with our reconstruction algorithm within a 3×3 Hilbert space choice ($N = 2$) lead to the reconstructed joint photon distribution shown in Fig. 3: here we can appreciate how the only relevant entries are ϱ_{01} and ϱ_{10} (single photon transmitted or reflected by the beam splitter), in good agreement with the inserted BS ratio.

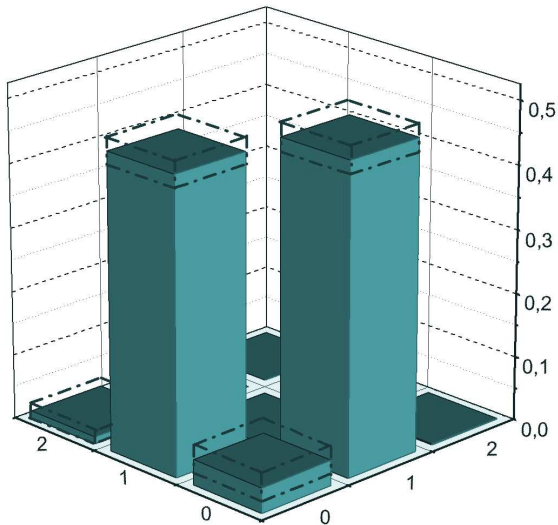


FIG. 3: On/off reconstruction of two-mode states. The plot shows the reconstructed ϱ_{nk} entries of the joint photon distribution of our $|\psi_{BS}\rangle$ for the setup with 50%-50% BS and 10 nm FWHM IF.

There is also a small nonzero vacuum component ϱ_{00} which is due to a non perfect background evaluation and subtraction in the experimental data and perhaps to some light absorption in the system caused by the BS cube. An additional test has been performed with the same BS but with different optical filters (red glass (RG) filters with $\lambda_{cut-off} = 750$ nm) in order to explore a different range of frequencies. The overall quantum efficiency in this experiment is $\eta = 0.088$, and the acquisition has been repeated with $K = 33$ decreasing values. Effective reconstruction of the photon distribution has been obtained also in this case. Then we replaced the 50%-50% BS cube with an unbalanced 60%-40% BS plate, maintaining the RG large band filters: with this setup we have an overall quantum efficiency $\eta = 0.0123$, and have performed $K = 41$ data collection. The difference between the transmitted and reflected branch of the BS was evident and in agreement with the known beam splitter ratio, with the only nonzero ϱ_{nk} being ϱ_{10} and ϱ_{01} . Finally, for the last test we have replaced the RG filters with the previous IF ones and obtain a similar results, i.e. excellent reconstruction of the joint photon distribution.

As a second example we consider the two-mode state obtained by inserting a single branch of type-I PDC emission without triggering, which corresponds to a multi-thermal multi-photon state [6], into a balanced beam splitter. In a setup similar to the previous one, [42], we have generated PDC light by means of a $5 \times 5 \times 5$ mm Type-I BBO crystal pumped by a Q-switched (triplicated to 355 nm) Nd:Yag laser with 5 ns pulses, power up to 200 mJ per pulse and 10 Hz repetition rate. Because of the very high power of the pump beam, a state with a large number of photon is generated for each pulse. We have therefore attenuated (by using 1 nm FWHM IF and neutral filters) the multithermal state before sending it to the BS and then detecting both the outgoing beams. Again, different quantum efficiencies are obtained by inserting (before the BS) Schott neutral filters, whose calibration is obtained by measuring the power of a diode laser before and after them, with the calibration laser injected in the same point as the PDC in order to minimize the effect due to eventual non homogeneous NF filters. The coincidence scheme is realized sending two Q-switch triggered pulses to two TAC modules as start inputs, and the APDs outputs as stop. Then, having set properly the 20 ns coincidence window, we address the two TAC outputs to the AND logic port, and the valid stops to the counting modules (together with one TAC's valid start and the AND output). The background is estimated and subtracted in the same way as in the previous experiment. The maximum quantum efficiency in this experiment has been evaluated by multiplying the APDs nominal quantum efficiencies, the IF peak transmittance and the fiber couplers effective efficiency, measured with the diode laser leading to $\eta = 0.25$. The expected on/off

joint statistics for this optical state is:

$$\begin{cases} p_{00}^\eta = [M(M + \eta N_{ave})^{-1}]^M \\ p_{01}^\eta = [M(M + \eta\tau N_{ave})^{-1}]^M - p_{00}^\eta \\ p_{10}^\eta = \{M[M + \eta(1 - \tau)N_{ave}]^{-1}\}^M - p_{00}^\eta \end{cases} \quad (21)$$

where N_{ave} is the average number of photons, M the number of propagation modes and τ the BS transmittance. The reconstructed joint photon statistics (now upon a 17×17 truncated Hilbert space) have been compared with the expected two-mode multithermal distribution

$$\varrho_{nm} = \frac{(n + m + M - 1)!}{n!m!(M - 1)!} \cdot \frac{\left(1 + \frac{N_{ave}}{M}\right)^{-M}}{\left(1 + \frac{M}{N_{ave}}\right)^{m+n}} \quad (22)$$

and the calculated fidelity is larger than $G \simeq 0.99$ for $i \geq 2000$. Overall, this experiment confirms of the reliability of our method, even when it is dealing with a larger Hilbert space and more intense beams, corresponding to quantum states with a larger number of photons.

IV. FULL STATE RECONSTRUCTION BY ON/OFF PHOTODETECTION

The method described in the previous Sections may provide the complete information on a quantum optical state when the density matrix of such a state is diagonal, i.e. all the off-diagonal elements are equal to zero. Of course, in real systems, it often occurs that also off-diagonal elements are relevant and a question arises on whether the on/off method may be generalized to obtain a more general procedure providing the reconstruction of the whole density matrix. In turn, the answer is positive, and basically require to supplement the on/off method with some additional phase information. Before entering into the details of our implementation let us consider a generic single-mode state, mixed with a strong coherent state, from now on the local oscillator (LO), in an unbalanced beam-splitter, i.e. high transmittance and low reflectance. In this case then the transmitted mode is *displaced* [50], i.e. it is equivalent to the signal mode shifted by a displacement operator $D(\alpha) = \exp(\alpha a^\dagger - \alpha^* a)$, where a (a^\dagger) is the photon destruction (creation) operator associated to the signal mode and $\alpha = |\alpha| e^{i\varphi}$ is the local oscillator field amplitude rescaled by the BS reflectance. If one measures the photon distribution of the transmitted beam, this corresponds to measuring the displaced Fock-state probability distribution of the original signal, i.e.

$$p_n(\alpha) = \langle n, \alpha | \rho | n, \alpha \rangle \quad (23)$$

where $|n, \alpha\rangle \equiv D(\alpha)|n\rangle$ are the displaced Fock states and ρ is the signal mode density operator. Note that p_n is now a function of the displacement α also.

The on/off state reconstruction method is, in turn, based on the above equation [51]. In fact, upon truncating the Hilbert space at dimension n_0 we can expand eq. 23 as follows

$$p_n(\alpha) = \sum_{k,m=0}^{n_0} \langle n, \alpha | k \rangle \langle k | \rho | m \rangle \langle m | n, \alpha \rangle \quad (24)$$

Expressing the displaced Fock states $|n, \alpha\rangle$ in the ordinary Fock basis, one obtains[51]:

$$p_n(\alpha) = e^{-|\alpha|^2} n! \sum_{k,m=0}^{n_0} \sqrt{k!m!} \langle k | \rho | m \rangle \times \sum_{j=0}^{\bar{j}} \sum_{l=0}^{\bar{l}} \frac{(-1)^{j+l} |\alpha|^{m+k+2(n-j-l)} e^{i(m-k)\varphi}}{j!(n-j)!(k-j)!l!(n-l)!(m-l)!} \quad (25)$$

where $\bar{j} \equiv \min\{n, k\}$ and $\bar{l} \equiv \min\{n, m\}$. Now, we assume $|\alpha|$ fixed, so that for any value of $|\alpha|$, $p_n(\alpha)$ can be regarded as a function of φ and expanded in a Fourier series, the general component being:

$$\begin{aligned} p_n^{(s)}(|\alpha|) &= \frac{1}{2\pi} \int_0^{2\pi} p_n(\alpha) e^{is\varphi} d\varphi \\ &= \sum_{m=0}^{n_0-s} G_{n,m}^{(s)}(|\alpha|) \langle m + s | \rho | m \rangle \end{aligned} \quad (26)$$

with:

$$\begin{aligned} G_{n,m}^{(s)}(|\alpha|) &= e^{-|\alpha|^2} n! \sqrt{m!(m+s)!} \times \\ &\times \sum_{j=0}^{\tilde{j}} \sum_{l=0}^{\tilde{l}} \frac{(-1)^{j+l} |\alpha|^{2(m+n-j-l)+s}}{j!(n-j)!(m+s-j)!l!(n-l)!(m-l)!} \end{aligned} \quad (27)$$

where $\tilde{j} \equiv \min\{n, m + s\}$. We notice that $p_n^{(s)}(|\alpha|)$ is related to the density matrix element whose row and column indices differ by s . If the photon number distribution $p_n(\alpha)$ is measured for $n = 0, 1, \dots, N$, with $N \geq n_0$, then Eq. (26) represents, for each fixed value of s , a system of $(N + 1)$ linear equations connecting the $(N + 1)$ measured quantities $p_n^{(s)}$ to $(n_0 + 1 - s)$ unknown density matrix elements. This system is clearly overdetermined, so it can be inverted using the least squares method in order to obtain the density matrix elements from the measured probabilities. The reconstructed off-diagonal density matrix elements can thus be obtained as:

$$\langle m + s | \rho_{rec} | m \rangle = \sum_{n=0}^N F_{n,m}^{(s)}(|\alpha|) p_n^{(s)}(|\alpha|) \quad (28)$$

where

$$F_{n,m}^{(s)}(|\alpha|) = \{[G_{n,m}^{(s)}(|\alpha|)]^T G_{n,m}^{(s)}(|\alpha|)\}^{-1} [G_{n,m}^{(s)}(|\alpha|)]^T \quad (29)$$

is the generalized Moore-Penrose inverse of G . The F matrix satisfies the condition:

$$\sum_{n=0}^N F_{m',n}^{(s)}(|\alpha|)G_{n,m}^{(s)}(|\alpha|) = \delta_{m,m'} \quad (30)$$

for $m, m' = 0, 1, \dots, n_0 - s$, so that from the exact probabilities the correct density matrix elements are found ($\rho_{rec} \equiv \rho$). Furthermore, the least squares method ensures that the $*p_n^{(s)}$ calculated from ρ_{rec} according to eq. (26) best fits the measured quantities such that $\sum_{m=0}^N (*p_n^{(s)} - p_n^{(s)})^2$ is minimized. In conclusion, upon combining Eqs. (28) and (26), we find out the formula for the direct sampling of the density matrix from the measured photon number distribution of the displaced state[51]:

$$\langle m + s | \rho_{rec} | m \rangle = \frac{1}{2\pi} \sum_{n=0}^N \int F_{n,m}^{(s)}(|\alpha|) e^{is\varphi} p_n(\alpha) d\varphi \quad (31)$$

It is worth mentioning that this method, given that the $p_n(\alpha)$ are known, requires only the value of φ to be varied.

Let us now extend our method to the case of imperfect photodetection with nonunit quantum efficiency η . The measured photodistribution $P_k(\alpha)$ is related to the actual photon number distribution $p_n(\alpha)$ by a Bernoullian convolution

$$P_k(\alpha) = \sum_{n=0}^{\infty} M_{k,n}(\eta) p_n(\alpha) \quad (32)$$

where $M_{k,n}(\eta)$ is:

$$M_{k,n}(\eta) = \begin{cases} \binom{n}{k} \eta^k (1-\eta)^{n-k} & k \leq n \\ 0 & k > n \end{cases} \quad (33)$$

The analogue of Eq.(26) for the measured quantities $P_n^{(s)}(|\alpha|)$ is given by

$$P_n^{(s)}(|\alpha|) = \sum_{m=0}^{n_0-s} G_{n,m}^{(s)}(|\alpha|, \eta) \langle m + s | \rho | m \rangle, \quad (34)$$

where the new matrices

$$G_{n,m}^{(s)}(|\alpha|, \eta) = \sum_{k=0}^{\infty} M_{n,k}(\eta) G_{k,m}^{(s)}(|\alpha|), \quad (35)$$

are obtained from the $G_{k,m}^{(s)}(|\alpha|)$, as defined in Eq. (27), and can be inverted in the same way described above to obtain some matrices $F_{m,n}^{(s)}(|\alpha|, \eta)$ to be used, as in Eq. (31), to reconstruct the whole density matrix.

The key element to realize the above method and, in turn, to achieve the reconstruction of the off-diagonal elements of the density matrix, is an interferometric setup where the signal mode and the local oscillator are mixed

in an unbalanced beam splitter. In practice, a source beam is sent to a Mach-Zehnder interferometer in which the part reflected by the first beam splitter is taken as the signal, while the transmitted portion is regarded as the local oscillator. The two modes are then mixed by the second beam splitter, which is effectively used to perform a sort of unbalanced homodyning. Upon changing the length of the optical path in the one arm of the interferometer, one may tune the relative phase between the signal mode and the local oscillator. In this way, one may measure the distributions $p_n(\alpha)$ at fixed $|\alpha|$ and for different phases. Besides, upon performing some action on the signal mode, one may also apply the reconstruction method to different input states. In the following, we report the results for the reconstruction of a coherent state and for a thermal state obtained by inserting a rotating glass plate in the path of the signal beam.

In our set-up [52], see Fig.4, the output of a He-Ne laser ($\lambda = 632.8$ nm) is lowered to the single photon regime by neutral filters. The spatial profile of the signal is the purified from non-Gaussian components by a spatial filter realized by two converging lenses and a $100 \mu\text{m}$ diameter wide pinhole. An iris just after the pinhole ensures the selection of a single Gaussian spatial mode. The laser cavity is also preserved by back-reflections, which may cause instability, by means of an optical isolator consisting in a Faraday rotator between two polarizers. The second polarizer (say, B) angle is shifted by 45° with respect to the first one (A), so that the light transmitted by the latter, whose polarization is rotated by 45° by the Faraday rotator, is all transmitted also by the second. Since the polarization rotation by Faraday effect is in the same direction regardless of the laser propagation direction, any back-reflected light passing through B, would suffer another 45° rotation before reaching a polarizer and would thus be stopped, being orthogonal to the polarizer angle.

After a beam-splitter, part of the beam is addressed to a control detector in order to monitor the laser amplitude fluctuations, while the remaining part is sent to the interferometer, its main structure consisting in a single invar block custom designed and developed at INRIM. A PI piezo-movement system allows to change the phase between the two paths by driving the position of the reflecting prism with nanometric resolution and high stability. For each position of the prism, the off events are collected for different sets of neutral filters, and thus, for different quantum efficiencies. The detector, a Perkin-Elmer Single Photon Avalanche Photodiode (SPCM-AQR), is gated by a 20 ns wide time window with a repetition rate of 200 kHz. In order to obtain a reasonable statistics, a single run consists of 5 repetitions of 4 second acquisitions. Events are recorded by a NI-6602 PCI counting module. In this case, since all the attenuations in front of the detectors can be included in the generation of the state, the overall maximum quantum efficiency is assumed to be 0.66, as the nominal efficiency declared by the manufacturer data-sheet of the photodetectors. As

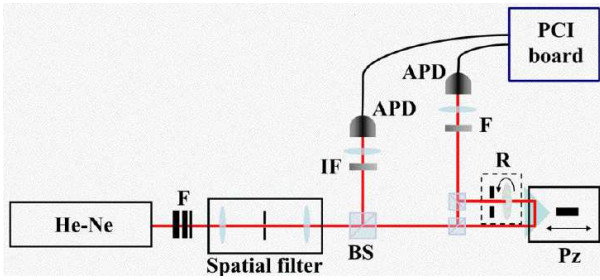


FIG. 4: Setup for the reconstruction of the density matrix for a coherent and a pseudo-thermal state. The emission of a He-Ne laser ($\lambda = 632.8$ nm) is lowered to single photon regime by neutral filters. A spatial filter realized by two converging lenses and a $100 \mu\text{m}$ diameter-wide pinhole purifies the shape of the signal and allows to select a single spatial mode. A beam-splitter reflects part of the beam to a control detector used to monitor the laser amplitude fluctuations, while the remaining part is sent to the interferometer. The phase between the "short" and "long" paths in the interferometer can be changed by driving the position of the reflecting prism by means of a PI piezo-movement system. A set of variable neutral filters allows to collect photons for different values of the quantum efficiency. The element in the dotted box is a rotating glass plate which is inserted in the setup only for the generation of the pseudo-thermal state. The detectors used are Perkin-Elmer Single Photon Avalanche Photodiode (SPCM-AQR) gated by a 20 ns wide time window with (repetition rate = 200 kHz). A single run consists of 5 repetitions of 4 seconds acquisitions and events are recorded by a NI-6602 PCI counting module.

said before, in another set of measurements, a rotating glass plate was inserted in the path of the signal in order to reconstruct a pseudo-thermal state.

In Fig. 5 we report the reconstructed density matrix in the Fock representation (diagonal and subdiagonal) for a coherent state with real amplitude $z \simeq 1.8$ and a thermal state with average number of photons equal to $n_{th} \simeq 1.4$. As it is apparent from the plots, the off-diagonal elements are correctly reproduced in both cases despite the limited visibility. Here the raw data are frequencies of the off event (see Fig. reffig:preresults2) as a function of the detector efficiency, taken at different phase modulations ϕ , whereas the intermediate step corresponds to the reconstruction of the photon distribution for the phase-modulated signals. In Fig. 6 we report the frequencies of the off events and the reconstructed photon distributions at the minimum and maximum of the interference fringes. In our experiments we used $N_\phi = 12$ and $|\alpha|^2 = 0.01$ for the coherent state and $|\alpha|^2 = 1.77$ for the thermal state. The use of a larger N_ϕ would allow the reliable reconstruction of far off-diagonal elements, which has not been possible with the present configuration. Work along these lines is in progress and results will be reported elsewhere.

The evaluation of uncertainties on the reconstructed states involves the contributions of experimental fluctuations of on/off frequencies as well as the statistical fluctuations

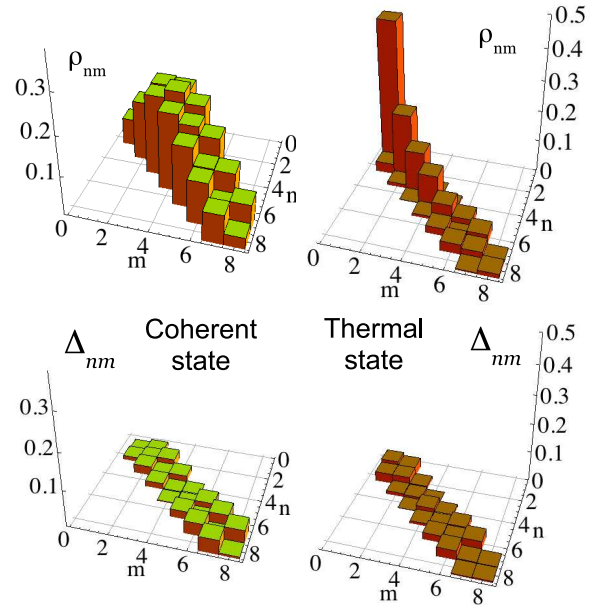


FIG. 5: State reconstruction by phase-modulation and on/off measurements. In the upper plots we report the reconstructed density matrix in the Fock representation (diagonal and subdiagonal elements) for the signal excited in a coherent state with real amplitude $z \simeq 1.8$ (left) and a thermal state with average number of photons equal to $n_{th} \simeq 1.4$ (right). In the lower plots we show the absolute difference $\Delta_{nm} = |\varrho_{nm}^{exp} - \varrho_{nm}^{th}|$ between reconstructed and theoretical values of the density matrix elements for the signal excited in a coherent (left) or a thermal (right) state.

tions connected with photon-number reconstruction. It has been argued [54, 55] that fluctuations involved in the reconstruction of the photon distribution may generally result in substantial limitations in the information obtainable on the quantum state, e.g. in the case of multip peaked distributions [56]. For our purposes this implies that neither large displacement amplitudes may be employed, nor states with large field and/or energy may be reliably reconstructed, although the mean values of the fields measured here are definitely non-negligible. On the other hand, for the relevant regime of weak field or low energy, observables characterizing the quantum state can be safely evaluated. In our experiments, the absolute errors $\Delta_{nm} = |\varrho_{nm}^{exp} - \varrho_{nm}^{th}|$ on the reconstruction of the density matrix in the Fock basis are reported in Fig. 5. Notice also that any uncertainty in the nominal efficiency of the involved photodetectors does not substantially affect the reconstruction in view of the robustness of the method to this kind of fluctuations [31].

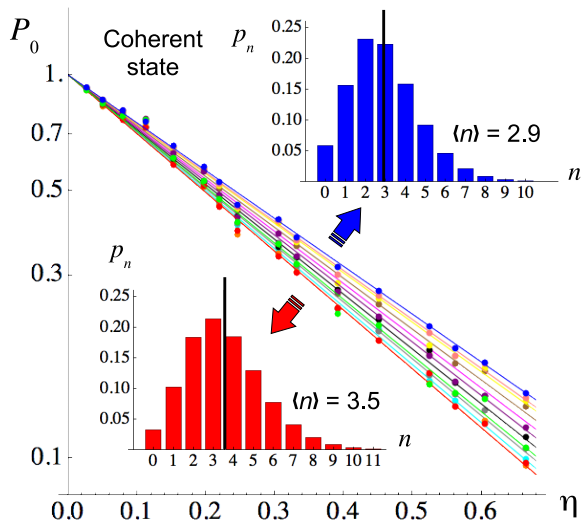


FIG. 6: State reconstruction by phase-modulation and on/off measurements. In the main plot we report the off frequencies as a function of the quantum efficiency as obtained when the signal under investigation is a coherent state and for different phase-shifts. The two insets show the reconstructed photon distributions for the two phase-modulated versions of the signal corresponding to maximum and minimum visibility at the output of the Mach-Zehnder interferometer. The vertical black bars denote the mean value of the photon number for the two distributions, $\langle a^\dagger a \rangle = 3.5$ and $\langle a^\dagger a \rangle = 2.9$.

V. CONCLUSIONS AND OUTLOOKS

In this paper we gave a panorama of the status of the art about the characterization of optical states by means of on/off photodetection. We have briefly reviewed the theoretical basis of the on/off method, and have reported the main recent experimental results for the reconstruction of the diagonal elements of single- and two-mode states, as well as for the reconstruction of the full density matrix of single-mode states. The on/off reconstruction method has been now tested in several optical regimes and it proved both effective and statistically reliable. This prompts to further applications of the scheme as a tool for the characterization at quantum level. In fact, we are currently going to apply the on/off method as an advanced characterization of detectors, i.e. for the reconstruction of their probability operator-valued measures (POVMs).

Acknowledgements

This work has been supported by EU project QuCandela, by Compagnia di San Paolo, by the MIUR projects PRIN 2007FYETBY and PRIN2005023443, by Regione Piemonte (E14) and by the CNR-CNISM agreement. MGAP thanks Zdenek Hradil, Maria Bondani, and Simone Cialdi for useful discussions.

-
- [1] D. Bouwmeester, A. Ekert and A. Zeilinger Eds., *The Physics Of Quantum Information*, Springer, Berlin-Heidelberg, (2000);
- [2] M. Genovese, *Phys. Rep.* 413, 6 (2005);
- [3] W. Vogel and D.G. Welsch, *Quantum Optics - An Introduction*, Wiley-VCH, Berlin, (2001);
- [4] W.P. Schleich, *Quantum Optics In Phase Space*, Wiley-VCH, Berlin, (2001);
- [5] J. Perina, Z. Hradil and B. Jurco, *Quantum Optics and Fundamental Physics*, Kluwer, Dordrecht, (1994);
- [6] L. Mandel and E. Wolf, *Optical Coherence And Quantum Optics*, Cambridge Univ. Press, Cambridge, (1995);
- [7] D. T. Smithey, M. Beck, M. G. Raymer and A. Faridani, *Phys. Rev. Lett.* 70, 1244 (1993);
- [8] G. M. D'Ariano, C. Macchiavello and M. G. A. Paris, *Phys. Rev. A* 50, 4298 (1994);
- [9] M. G. Raymer and M. Beck, in *Quantum States Estimation*, Edited M. G. A. Paris and J. Rehacek, Springer, Berlin-Heidelberg, (2004), pp. 235-289;
- [10] G. M. D'Ariano, P. Lo Presti, in *Quantum States Estimation*, Edited M. G. A. Paris and J. Rehacek, Springer, Berlin-Heidelberg, (2004), pp. 297-319;
- [11] R. H. Hadfield, *Nature Photon.* 3, 696 (2009);
- [12] C. Silberhorn, *Contemp. Phys.* 48 (3), 143 (2007);
- [13] G. Zambra, M. Bondani, A. S. Spinelli and A. Andreoni, *Rev. Sci. Instrum.* 75, 2762 (2004);
- [14] G. A. Morton, *RCA Rev* 10, 525 (1949);
- [15] E. Hergert, in *Proceedings of the Single Photon Detector Workshop*, (2003), March 31- April 1; Gaithersburg, USA;
- [16] A. Fukasawa, J. Haba, A. Kajeyama, H. Nakazawa and M. Suyama, *IEEE Trans. Nucl. Sci.* 55, 758 (2008);
- [17] J. Kim, S. Takeuchi, Y. Yamamoto and H.H. Hogue, *Appl. Phys. Lett.* 74, 902 (1999);
- [18] G. Di Giuseppe, A.V. Sergienko, B.E.A. Saleh and M.C. Teich, in *Quantum Information and Computation*, Proceedings of the SPIE 5105, (2003), August 3; San Diego, CA, USA;
- [19] A. E. Lita, A. J. Miller and S. W. Nam, *Opt. Express* 16, 3032 (2008);
- [20] M. Munroe, D. Boggavarapu, M.E. Anderson and M.G. Raymer, *Phys. Rev. A* 52, R924 (1995);
- [21] J. B. Altepeter, D. F. V. James and P. G. Kwiat, *Quantum States Estimation*, in *Lect. Not. Phys.* 649, Springer, Berlin-Heidelberg, (2004);
- [22] G. M. D'Ariano, M. Rubin, M. F. Sacchi and Y. Shih, *Fortsh. Phys.* 48, 599 (2000);
- [23] A. I. Lvovsky and S. A. Babichev, *Phys. Rev. A* 66, 011802 (2002);
- [24] M. Vasilyev, S. K. Choi, P. Kumar and G. M. D'Ariano, *Phys. Rev. Lett.* 84 (11), 2354 (2000);
- [25] A. I. Lvovsky, H. Hansen, T. Aichele, O. Benson, J. Mlynek and S. Schiller *Phys. Rev. Lett.* 87 (5), 050402 (2001);

- [26] F. Zappa, A.L. Lacaita, S.D. Cova and P. Lovati, *Opt. Eng.* 35, 938 (1996);
- [27] S. Cova, M. Ghioni, A. Lotito, I. Rech and F. Zappa, *J. Mod. Opt.* 51, 1267 (2004);
- [28] R. G. W. Brown, R. Jones, K. D. Ridley and J. G. Rarity, *Appl. Opt.* 26, 2383 (1987);
- [29] D. Mogilevtsev, *Opt. Comm* 156, 307-310, (1998);
- [30] D. Mogilevtsev, *Acta Phys. Slov.* 49, 743-748, (1999);
- [31] A.R. Rossi, S. Olivares and M.G.A. Paris, *Phys. Rev. A* 70, 055801, (2004);
- [32] A.R. Rossi and M.G.A. Paris, *E. Phys. Jour. D* 32, 223-226 (2005);
- [33] D. Achilles, C. Silberhorn, C. Sliwa, K. Banaszek and I. A. Walmsley, *J. Mod. Opt.* 51 1499 (2004);
- [34] P. P. Rohde, *J. Opt. B: Quantum Semiclass. Opt* 7, 82 (2005);
- [35] M. J. Fitch, B. C. Jacobs, T. B. Pittman and J. D. Fran-son *Phys. Rev. A* 68, 043814 (2003);
- [36] Z. Hradil, D. Mogilevtsev and J. Rehacek, *Phys. Rev. Lett.* 96, 230401 (2006);
- [37] J. Rehacek, D. Mogilevtsev, Z. Hradil, *Phys. Rev. Lett.* 105, 010402 (2010);
- [38] G. Zambra, A. Andreoni, M. Bondani, M. Gramegna, M. Genovese, G. Brida, A. Rossi and M. G. A. Paris, *Phys. Rev. Lett.* 95, 063602/1-4 (2005);
- [39] M. Genovese, G. Brida, G. Zambra, A. Andreoni, M. Bondani, M. Gramegna, A. Rossi and M. G. A. Paris, *Laser Physics* 16, 385-392 (2006);
- [40] G. Brida, M. Chekhova, M. Genovese, M. Gramegna, L. A. Krivitsky, M. L. Rastello, *Journ. of Opt. Soc. of Am. B* 22, 488 (2005);
- [41] G. Brida, M. Genovese, M. Gramegna, M. G. A. Paris, E. Predazzi and E. Cagliero, *Open Syst. & Inf. Dyn.* 13, 333-341 (2006);
- [42] G. Brida, M. Genovese, M.G.A. Paris and F. Piacentini, *Opt. Lett.* 31, Issue 23 (2006);
- [43] G. Brida, M. Genovese, M. G. A. Paris, F. Piacentini, E. Predazzi and E. Vallauri, *Opt. & Spect.* 103, 95 (2007);
- [44] T. Moroder, M. Curty and N. Ltkenhaus, *New J. Physics*, 11, 045008 (2009);
- [45] A. P. Dempster, N. M. Laird and D. B. Rubin, *J. R. Statist. Soc. B* 39, 1 (1977);
- [46] G. Brida, M. Genovese, A. Meda, S. Olivares, M. G. A. Paris and F. Piacentini, *Journ. Mod. Opt.* 56, 196 (2009);
- [47] G. Brida, N. Antonietti, M. Genovese, M. Gramegna, L. A. Krivitsky, F. Piacentini, M. L. rastello, I. Ruo Berchera, P. Traina, *Int. J. Quant. Inf.* 5, 1-2, 265-272 (2007);
- [48] G. Brida, M. Genovese and C. Novero, *J. Mod. Opt.* 47, 2099 (2000);
- [49] G. Brida, M. Genovese and M. Gramegna, *Las. Phys. Lett.* 3, 115 (2006);
- [50] M. G. A. Paris, *Phys. Lett. A*, 217, 78 (1996);
- [51] T. Opatrný and D.-G. Welsh, *Phys. Rev. A* , 55, 1462 (1997);
- [52] A. Allevi, A. Andreoni, M. Bondani, G. Brida, M. Genovese, M. Gramegna, P. Traina, S. Olivares, M. G. A. Paris and G. Zambra, *Phys. Rev. A* 80, 022114 (2009);
- [53] G. Brida, M. Genovese, M. Gramegna, M. Gramegna, P. Traina, E. Predazzi, S. Olivares and M. G. A. Paris, *Int. J. Quant. Inf.* 7, 27 (2009);
- [54] K. Banaszek and K. Wodkiewicz, *J. Mod. Opt.* 44, 2441 (1997);
- [55] K. Banaszek, *J. Mod. Opt.* 46, 675 (1999);
- [56] G. Zambra and M. G. A. Paris, *Phys. Rev. A* 74, 063830 (2006);